driven networks exhibit simple aging, characterized by a unique relevant time scale. On the other hand, the case $\gamma > 1$ corresponds to a more complex picture, with several competing characteristic time scales.

We have organized our manuscript as follows: In Sec. 2 we recall the definition of the activity driven model. Sec. 3 defines the continuous time implementation of directed random walks on activity driven networks and derives the analytic steady state solution for the occupation probability in terms of a generalized Montroll-Weiss equation. In Sec. 4 we present numerical evidence for the aging behavior of the occupation probability $P(a,t)$, defined as the probability that the walker is in a node of activity a at time t. In Sec. 5 we develop the mapping of the random walk process to Bouchaud's trap model. The mapping suggests additional quantities characterizing the aging behavior of the system, which are numerically analyzed. Our conclusions are finally presented in Sec. 6.

2 The activity driven network model

The activity driven network model [23,27] is defined as follows: N nodes (individuals) in the network are endowed with an activity $a_i \in [\varepsilon, 1]$, extracted randomly from an activity distribution $F(a)$. Every time step $\Delta t = 1/N$, an agent i is chosen uniformly at random. With probability a_i, the agent becomes active and generates m links that are connected to m other agents, chosen uniformly at random. Those links last for a period of time Δt (i.e. are erased at the next time step). Time is updated by $t \to t + \Delta t$. For simplicity, we will consider in the following $m = 1$. The topological properties of the integrated network at time t (i.e. the network in which nodes i and j are connected if there has ever been a connection between them at any time $t' \leq t$) have been studied in Ref. [27], obtaining as a main result that the integrated degree distribution at time t, $P_t(k)$, scales in the large t limit as the activity distribution, i.e.

$$P_t(k) \sim t^{-1} F\left(\frac{k}{t} - \langle a \rangle\right). \tag{1}$$

Empirical measurements report activity distributions in real temporal networks exhibiting long tails of the form $F(a) \sim a^{-\gamma}$ [23]. This expression thus relates in a simple way the functional form of the activity distribution and the degree distribution of the integrated network at time t, and allows to explain the scale-free form of the latter observed in social networks [28,29].

In this paper we will consider activity distributions with this power-law form. The range of values of the a is restricted to $a \in [\varepsilon, 1]$, where a minimum activity ε is set to avoid divergencies close to zero. The normalized form of the distribution thus depends on the value of γ:

$$F(a) = \frac{1-\gamma}{1-\varepsilon^{1-\gamma}}\, a^{-\gamma}. \tag{2}$$

As we will see later, the parameter ε will play a significant role in the analysis of random walks on activity driven networks.

3 Random walks on activity driven networks

The dynamics of a random walk on activity driven networks is defined as follows [20,21,22]: A walker arriving at a node j at time t remains on it until an edge is created joining i and other node j at a subsequent time $t' > t$. The walker then jumps instantaneously to node j and waits there until an edge departing from it is created. To simplify calculations, here we will focus on *activated random walks*: a walker can leave node i only when i becomes active and creates an edge pointing at another node [20]. Once the walker has arrived to node i, it must wait there until i creates a new connection. Since i creates new edges with constant probability a_i per unit time, the walker will remain trapped in i for a number of time steps n given by the exponential distribution, $\psi_i(n) = \frac{a_i}{N}\left(1 - \frac{a_1}{N}\right)^{n-1}$, independently of the time of the last activation of i. In the limit of large N we can take the continuous time limit and define a *waiting time* $\tau = n/N$, which is given by a local waiting time distribution

$$\psi_{a_i}(\tau) = a_i e^{-a_i \tau}. \tag{3}$$

That is, the dynamics of hopping from one node to another, follows in time a Poisson process with a rate a_i that depends on node i.

The dynamics of activated random walks under this restriction is particularly easy to implement in continuous time: Considering that the walker is at vertex i with activity a_i at time t, it hops to a randomly selected node j and time is updated as $t \to t + \tau$, where τ is a random variable extracted from the distribution Eq. (3). This continuous time implementation has the additional benefit of not restricting the maximum possible value of the activity a, which can be now considered as a probability rate. With this definition, a directed random walk on an activity driven netwok can be directly mapped to a continuous time random walk (CTRW) on a fully connected network in which each node has a different distribution of waiting times $\psi_i(\tau)$ [18].

3.1 Steady state solution

The time evolution of the activated random walk on activity driven networks can be studied by means of the generalized Montroll-Weiss equation approach [18,22]. For a Poissonian waiting time distribution, as in Eq. (3), the occupation probability $P(i,t)$ of finding the walker in node i at time t fulfills the exact equation [22]

$$\frac{dP(i,t)}{dt} = -\Lambda_i P(i,t) + \sum_j \lambda_{ij} P(i,t), \tag{4}$$

where λ_{ij} is the probability per unit time that the walker jumps from node j to node i, and $\Lambda_j = \sum_i \lambda_{ij}$ is the probability per unit time that the walker at j leaves this node. For the activated random walk on activity driven

networks, we obviously have $\lambda_{ij} = a_j/N$ and $\Lambda_j = a_j$. Eq. (4) then reads

$$\frac{dP(i,t)}{dt} = -a_i P(i,t) + \frac{1}{N}\sum_j a_j P(j,t). \qquad (5)$$

We can obtained an effective equation for the probability $P(a,t)$ that the walker is in a node of activity a at time t by performing a coarse-graining of Eq. (5), in which we define $P(a,t) = \sum_{i\in\mathcal{V}(a)} P(i,t)$, where $\mathcal{V}(a)$ is the set of nodes with activity a, with an average size $N_a = NF(a)$. Applying this definition on Eq. (5), and rearranging the summation over j, we obtain

$$\frac{dP(a,t)}{dt} = -aP(a,t) + F(a)\sum_{a'} a' P(a',t). \qquad (6)$$

From Eq. (6) it is straightforward to obtain the steady state solution $\lim_{t\to\infty} P(a,t) \equiv P_\infty(a)$ by imposing $\frac{dP(a,t)}{dt} = 0$, obtaining

$$P_\infty(a) = \frac{F(a)}{a}\sum_{a'} a' P_\infty(a') \equiv \frac{1}{\langle a^{-1}\rangle}\frac{F(a)}{a}, \qquad (7)$$

where in the last term we have applied the normalization condition $\sum_a P_\infty(a) = 1$, thus recovering the result obtained in Ref. [20].

4 Slow relaxation dynamics

Eq. (6) yields information about the occupation probability of nodes with activity a at large times, Eq. (7), expression whose accuracy has been checked numerically [20]. From it, however, it is hard to extract information about the time evolution of the process, and in particular, about the time scales of the relaxation to the steady state. We explore this issue by means of numerical simulations. Thus, in Fig. 1 we plot the occupation probability $P(a,t_w)$ of nodes of activity a, measured after letting the walker evolve for a time t_w. As Fig. 1 shows, the occupation probability exhibits a very slow relaxation from a state $P(a,t_w\to 0) \sim F(a)$ at short times to the equilibrium state, $P_\infty(a) \sim F(a)/a$, at large times, see Eq. (7). As a function of a for fixed t_w, this relaxation translates in a crossover between both scaling regimes at a crossover activity $a_c(t_w)$ which is a decreasing function of t_w.

We can understand the origin of this crossover by the following argument [30]: The average time τ_a to exit from a node with activity a is

$$\tau_a = \int_0^\infty \tau\psi_a(\tau) = \frac{1}{a}. \qquad (8)$$

A walker initially at a node of activity a, is expected to remain there for any time smaller than τ_a. Since the smallest activity in the network is ε, for $t_w > \varepsilon^{-1}$ the walker has had the chance to explore (and scape from) all nodes in the network, and therefore we expect to find it in

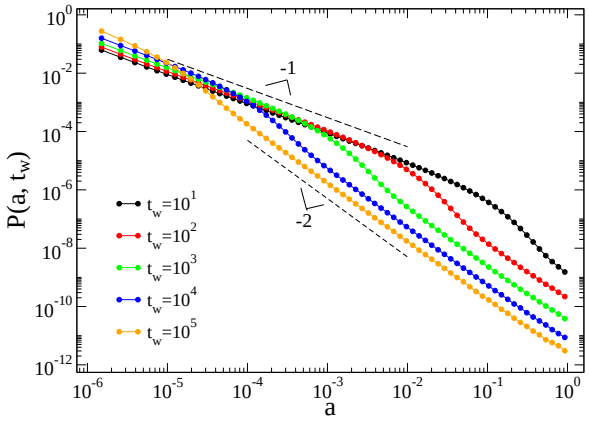

Figure 1. Evolution towards equilibrium of the occupation probability $P(a,t_w)$, measured after a time t_w, in activity driven networks with activity distribution $F(a) \sim a^{-\gamma}$, with $\gamma = 1$ and minimum activity $\varepsilon = 10^{-6}$. For small t_w, the occupation probability is proportional to the activity distribution, $P(a,t_w\to 0) \sim F(a) \sim a^{-1}$; for large t_w, it saturates to the steady state form $P(a,t_w\to\infty) = P_\infty(a) \sim F(a)/a \sim a^{-2}$. Network size $N = 5\times 10^6$.

the steady state. For any arbitrary time $t_w < \varepsilon^{-1}$, one can thus consider that all nodes with activity a such that $\tau_a < t_w$ (large a) will have had time to relax and reach the steady state, while nodes with activity fulfilling $\tau_a > t_w$ (small a) will not have relaxed. We thus see that the crossover activity fulfills $\tau_{a_c} \sim t_w$ or, from Eq. (8), $a_c(t_w) \sim t_w^{-1}$. The previous argument suggests therefore the following scaling form for the whole occupation probability:

$$P(a,t_w) = t_w\, \mathcal{P}(a\, t_w), \qquad (9)$$

where $\mathcal{P}(z)$ is a scaling function satisfying

$$\mathcal{P}(z) \sim \begin{cases} z^{-\gamma} & \text{for } z \ll 1 \\ z^{-\gamma-1} & \text{for } z \gg 1 \end{cases} \qquad (10)$$

This scaling regime is expected to hold for times $t_w < \varepsilon^{-1}$, i.e. before the full relaxation to the steady state.

In Fig. 2 we check the scaling form in Eq. (9) for activated random walks in activity driven networks with power-law activity distribution. For values of $\gamma < 1$, Fig. 2(a), we observe that the scaling form of the occupation probability is perfectly fulfilled for all times $t_w < \varepsilon^{-1}$. Surprisingly, however, the scaling form fares quite badly for $\gamma > 1$, performing increasingly worst for larger values of γ.

5 Mapping to Bouchaud's trap model and aging behavior

The radical difference in behavior of the random walk for γ larger or smaller than 1 can be understood in terms of a mapping to the well-known Bouchaud's trap model [25, 26] for glassy behavior (see also [30,31]). The trap model

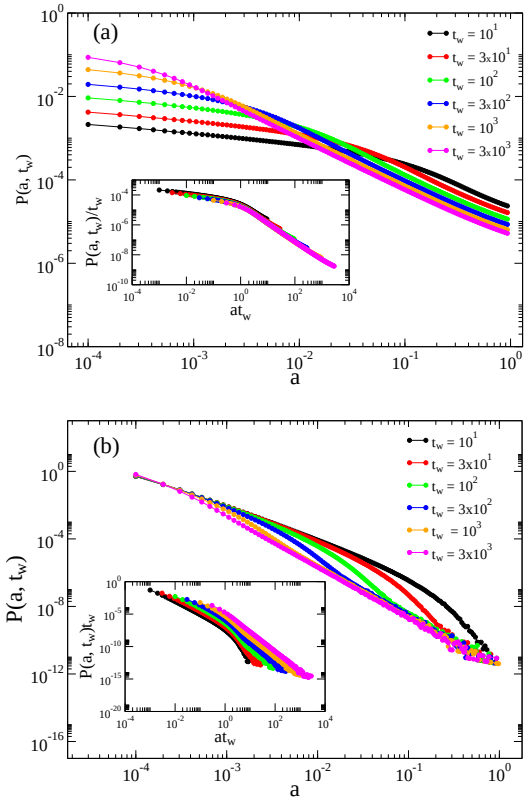

Figure 2. Occupation probability $P(a, t_w)$ as a function of the activity a at different times t_w. Data refer to activity-driven networks with $N = 5 \times 10^6$, $\varepsilon = 10^4$, and (a) $\gamma = 0.25$, (b) $\gamma = 2.00$. Insets: Data collapse according to the scaling form Eq. (9).

is defined in terms of a phase space consisting on N *traps*, each one with a depth E_i, $i = 1, \ldots, N$, extracted randomly from the probability distribution $\rho(E)$. The dynamics of the model proceeds by a succession of jumps between the traps, ruled by the temperature of the system, T. At this temperature, the system remains in a trap of depth E a random time τ distributed according to a Poisson process with rate $\tau_E^{-1} = \exp(-E/T)/\tau_0$, where τ_0 is a microscopic time scale that can be arbitrarily set equal to 1. After this time, the system jumps to a randomly chosen trap. Since all traps are equivalent, the probability that the system lands on a trap of depth E after a jump is $\rho(E)$. The average time spent in any trap is thus

$$\langle \tau \rangle = \int \rho(E) \tau_E \, dE. \tag{11}$$

The trap model exhibits a phase transition between a high temperature phase, where τ is finite, to a low temperature, glassy state characterized by very slow relaxation dynamics and aging behavior [24], when $\langle \tau \rangle$ diverges. This transition takes place at a finite temperature T_0 for a depth probability distribution of the form $\rho(E) = \exp(-E/T_0)$ [25,26], in which case the distribution of trapping times takes the form

$$P(\tau) \sim \tau^{-1-T/T_0} \tag{12}$$

For $T < T_0$, the exponent in the power-law in Eq. (12) is smaller than 2 and thus leads to an infinite average trapping time.

Activated random walkers can be easily mapped to the trap model by noticing the mapping between the respective jumping rates, that is

$$a = \tau_E^{-1} = \exp(-E/T), \tag{13}$$

form where we obtain the equivalence between depth and activity

$$E = -T \ln(a), \tag{14}$$

with a range of variation $E \in [0, T \ln(\varepsilon^{-1})]$. The relation between the activity distribution and the depth distribution is given by $\rho(E)\, dE = F(a)\, da$, leading to

$$\rho(E) = \frac{e^{-E/T}}{T} F\left(e^{-E/T}\right). \tag{15}$$

Assuming now an activity with a power-law distribution as is Eq. (2), we obtain

$$\rho(E) \sim \frac{1}{T} \exp\left[-(1-\gamma)E/T\right]. \tag{16}$$

Let us consider separately the different possible values of γ.

5.1 Case $\gamma < 1$

From Eq. (16), the mapping to the trap model makes perfect sense for $\gamma < 1$. In this case, $\rho(E)$ is a decreasing function of the depth E, corresponding to the presence of many shallow traps and a few deep ones. Deep traps represent rare long trapping events that eventually dominate the dynamics below the glass transition and induce a very slow relaxation and aging behavior [25,26]. In this case, however, temperature plays no role in the equivalent dynamics of the activated random walkers, as it can be absorbed in a change of variables $\bar{E} = E/T$, with a range of variation $\bar{E} \in [0, \ln(\varepsilon^{-1})]$. From the point of view of the mapping to the trap model, the activated random walker is a system in a fully glass state, corresponding to a infinite glass transition temperature. This can easily be seen by looking at the average waiting time distribution, i.e

$$\psi(\tau) = \sum_a F(a) a e^{-a\tau} \simeq \frac{1-\gamma}{1-\varepsilon^{1-\gamma}} \int_\varepsilon^\infty a^{1-\gamma} e^{-a\tau} da = \\ \simeq \tau^{-2+\gamma} e^{-\varepsilon\tau}, \tag{17}$$

where we have made an expansion for $\tau < \varepsilon^{-1}$. The exponent in Eq. (17) is always smaller than 2, indicative of an infinite glass transition temperature. The average trapping time is thus modulated by the exponential factor, diverging when $\varepsilon \to 0$, i.e. when the upper cut-off of the associated energy tends to infinity.

This analogy allows to explore in the random walk problem other features of the glassy dynamics of the trap model, in particular aging effects [24]. Aging effects are here usually measured by looking at the two-time correlation function $C(t;t_w)$, between the states of the system at times t_w and $t+t_w$. This correlation function, which is defined as the average probability that the system in a given trap at time t_w has not performed a jump at time $t+t_w$, fulfills in the trap model the scaling relation

$$C(t;t_w) = \mathcal{C}\left(\frac{t}{t_w}\right), \tag{18}$$

corresponding to the so-called "simple" aging [25,26]. This scaling can be simply deduced for the random walk on activity driven networks: Since the jumping dynamics is Poissonian in every node, the probability of not leaving a node with activity a in a time interval t is e^{-at}. We thus can write

$$\begin{aligned} C(t;t_w) &= \int_\varepsilon^1 P(a,t_w)e^{-at}\,da = \int_\varepsilon^1 t_w\mathcal{P}(a\,t_w)e^{-at}\,da \\ &= \int_{t_w\varepsilon}^{t_w} \mathcal{P}(z)e^{-zt/t_w}\,dz, \end{aligned} \tag{19}$$

where we have used the scaling relation Eq. (9) for $P(a,t_w)$ and performed a change of variable. For large z, the upper limit of the integral can be safely set equal to infinity, due to the exponential cut-off. In the limit of small z, we have $\mathcal{P}(z) \sim z^{-\gamma}$, and its integral also converges for $t_w\varepsilon$ small. Thus, in the double limit $1 \ll t_w \ll \varepsilon^{-1}$, we have

$$C(t;t_w) \simeq \int_0^\infty \mathcal{P}(z)e^{-zt/t_w}\,dz, \tag{20}$$

recovering the scaling relation for the correlation Eq. (18), which is expected to hold for waiting times $t_w \ll \varepsilon^{-1}$. In Fig. 3 we show that, for $\gamma < 1$, the scaling of the correlations is very well fulfilled in the random walk process.

Additional information on the aging properties of the system can be gathered by looking at the average escape time $t_{\rm esc}(t_w)$ that a walker at a given node at time t_w requires to escape from it [30]. In Fig. 4(inset) we plot the curves of the escape time as a function of t_w, for different values of ε. As we can see, the escape time is a increasing function of t_w for small values of t_w, indicating another of the typical features of aging systems, namely a breaking of scale invariance translation. Due to its Poissonian nature, the average time to leave a node with activity a is $\tau_a = 1/a$. Therefore, we can write $t_{\rm esc}(t_w) = \int da\; P(a,t_w)/a$. Applying the scaling relation Eq. (9) and performing a change of variables, we have

$$t_{\rm esc}(t_w) = t_w \int_{\varepsilon t_w}^{t_w} \frac{\mathcal{P}(z)}{z}\,dz. \tag{21}$$

For large t_w, the upper limit of the integral is not singular, and we can set it to infinity. We are therefore led to the scaling form

$$t_{\rm esc}(t_w) \simeq t_w\mathcal{F}(t_w\,\varepsilon), \tag{22}$$

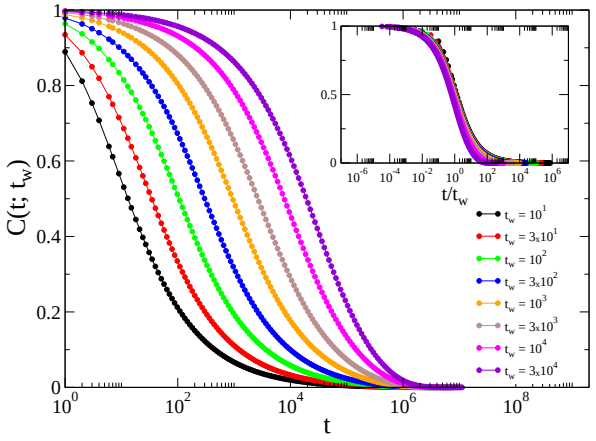

Figure 3. Two-time correlation function for random walks on activity driven networks with a power-law activity distribution. Data refers to $N = 5\times10^6$, $\gamma = 0.50$ and $\varepsilon = 10^{-6}$. Inset: Scaling plot corresponding to the form in Eq. (18).

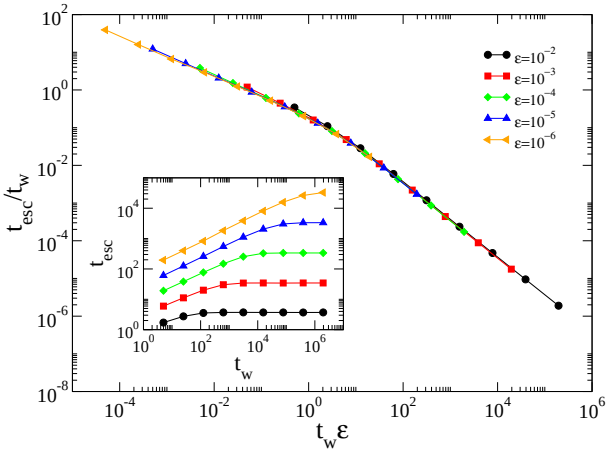

Figure 4. Scaling plot of the average scape time according to Eq. (22) for $\gamma = 0.50$. Inset: raw data. Data corresponds to a network size $N = 10^5$.

which is valid for $t_w \ll \varepsilon^{-1}$.

We check this theoretical predictions by means of a data collapse analysis, plotting $t_{\rm esc}(t_w)/t_w$ as a function of $t_w\varepsilon$. In Fig. 4(main) we plot the result, showing an excellent agreement with the prediction.

5.2 Case $\gamma > 1$

For the case $\gamma > 1$, Eq. (16) indicates that the mapping to the trap model is not physical. For this range of γ values, the density of traps *increases* with depth, meaning that very deep traps are much more probable than shallow ones. Long time trapping is thus not a rare event, but the norm of the system. This implies a qualitatively different, much slower dynamics than for the case $\gamma < 1$. This effect can be simply seen by looking at the coverage $S(t)$ of the random

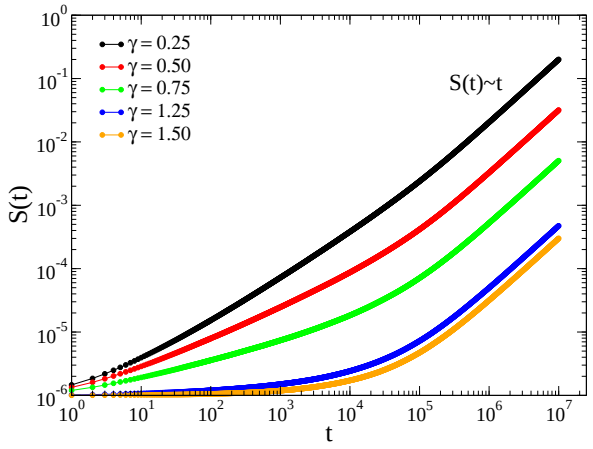

Figure 5. Coverage as a function of time. For $\gamma < 1$, dashed lines represent the predicted behavior $\sim t^{1-\gamma}$ from Eq. (26). We use $N = 10^6$ and $\varepsilon = 10^{-5}$.

walk as a function of time, defined as the average fraction of different nodes that a walker has visited up to time t, see Fig. 5. For very large $t > \varepsilon^{-1}$, the system has reached the steady state, and the walker jumps from any node at an average increment time $\Delta t = \langle \tau \rangle$, where the average waiting time $\langle \tau \rangle$ is defined as

$$\langle \tau \rangle = \int_{\varepsilon}^{1} F(a) \tau_a \, da = \langle a^{-1} \rangle = \frac{1-\gamma}{\gamma} \frac{\varepsilon^{-\gamma} - 1}{1 - \varepsilon^{1-\gamma}}, \qquad (23)$$

where we have used Eqs. (23) and (2). In this limit of large t, and since walker jumps to randomly chosen new nodes, we expect

$$S(t) \sim \frac{t}{\langle a^{-1} \rangle}, \quad t \gg \varepsilon^{-1}. \qquad (24)$$

For $\gamma < 1$ and short times, we observe a power law increase of the coverage, $S(t) \sim t^{\alpha}$. In the case $\gamma > 1$, on the other hand the initial growth is extremely slow, slower numerically than logarithmical, in the region $t < \varepsilon^{-1}$, where the dynamics is dominated by an exceedingly large number of deep traps. After this very slow regime, the linear, steady state behavior is recovered. We can explain the exponent of the initial growth of $S(t)$ for $\gamma < 1$ by the following argument: At any time $t \ll \varepsilon^{-1}$, the random walker will have explored in average nodes with activity restricted to $a > t^{-1}$, since it will not have had time to escape deeper traps. In this case, the average inverse activity of those nodes explored will depend on time as

$$\langle a^{-1} \rangle_t \sim \int_{t^{-1}}^{1} \frac{F(a)}{a} \, da \sim t^{\gamma}. \qquad (25)$$

We therefore estimate a coverage

$$S(t) \sim \frac{t}{\langle a^{-1} \rangle_t} \sim t^{1-\gamma}, \qquad (26)$$

with an exponent $\alpha = 1 - \gamma$ which is a decreasing function of γ, in agreement with the results in Fig. 5.

The anomalous density of deep traps for $\gamma > 1$ has a strong effect in the scaling of the occupation probability. In Fig. 2(b) we have plotted the function $P(a, t_w)$ for $\gamma = 2.0$. From the rescaled plot, it is evident that a simple scaling behavior such as the one represented in Eq. (9) is doomed to fail. In particular, as we can observe, the occupation probability for small values of a is apparently independent of t_w. This fact is in stark contrast with the behavior for $\gamma < 1$, Fig. 2(a), in which the value of $P(a, t_w)$ for small a increases for increasing t_w, as expected from Eq. (9). This phenomenology is again due to the anomalous abundance of deep traps in the region $\gamma > 1$: thus, while at t_w the walker has had the opportunity to explore and escape from nodes with activity $a > t_w^{-1}$, the fraction of such nodes is very small for large values of γ. Indeed, denoting by $\phi(t_w)$ the fraction of such nodes, we have

$$\phi(t_w) = \int_{t_w^{-1}}^{1} F(a) = \frac{1 - t_w^{\gamma-1}}{1 - \varepsilon^{1-\gamma}}. \qquad (27)$$

Denoting by $\phi^{>}(t_w)$ (resp. $\phi^{<}(t_w)$) the fraction corresponding to $\gamma > 1$ (resp. $\gamma < 1$), we have, in the limit of small ε,

$$\phi^{>}(t_w) \sim (t_w \varepsilon)^{\gamma-1}, \quad \phi^{<}(t_w) \sim 1 - t_w^{\gamma-1}. \qquad (28)$$

I.e. the fraction of visited nodes up to time t_w grows much faster for $\gamma < 1$ than in the opposite case.

While the scaling relation Eq. (9) is invalid for $\gamma > 1$, we can still understand the functional form of the occupation probability by means of the following argument: Let us consider a walker at time t_w. Initially, the walker starts at a randomly chosen node with activity a_0. With probability $e^{a_0 t_w}$, the walker does not move from its initial position, and therefore it contributes to the initial activity a_0. With the complementary probability $1 - e^{a_0 t_w}$, the walker has performed one or more jumps. Assuming that after its first jump it already reaches the steady state $F(a)/[a\langle a^{-a} \rangle]$, we have the average occupation probability

$$P(a, t_w) = F(a) e^{-a t_w} + \frac{F(a)}{a \langle a^{-1} \rangle} \left[1 - \int_{\varepsilon}^{1} e^{-a_0 t_w} F(a_0) \right].$$

For the activity distribution given by Eq. (2), we have

$$P(a, t_w) = F(a) e^{-a t_w} + \frac{F(a)}{a \langle a^{-1} \rangle} \times \\ \times \left[1 - \frac{1-\gamma}{1 - \varepsilon^{1-\gamma}} t^{-1+\gamma} \Gamma(1-\gamma, t_w \varepsilon) \right], \qquad (29)$$

where in the integral we have extended the upper limit up to infinity, and $\Gamma(a, z)$ is the incomplete Gamma function [32]. In Fig. 6 we plot the numerical data for $\gamma = 2$, compared with the theoretical prediction in Eq. (29). As we can see, except for very small values of the activity a, the fit of the theoretical prediction with the numerical results is excellent. The mixing of time scales in Eq. (29), namely a^{-1} and ε^{-1}, allows to understand the failure of the simple scaling ansatz performed to derive Eq. (9).

Finally, let us consider the average escape time $t_{esc}(t_w)$ for $\gamma > 1$. The lack of simple scaling evidenced in Eq. (29)

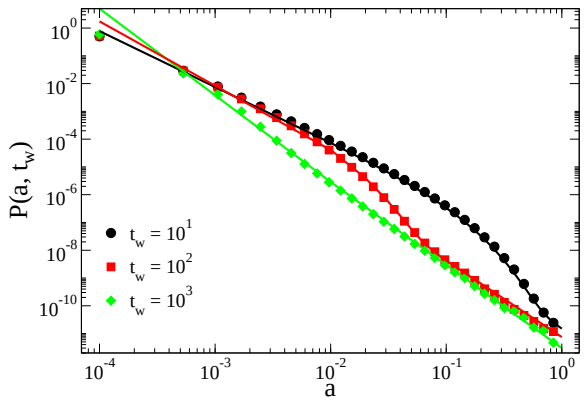

Figure 6. Evolution of the occupation probability $P(a,t)$. Data refer to activity-driven network with $N = 5 \times 10^6$, $\varepsilon = 10^4$, $\gamma = 2.00$, and different waiting times t_w. Solid lines are non-linear regressions using Eq. (29).

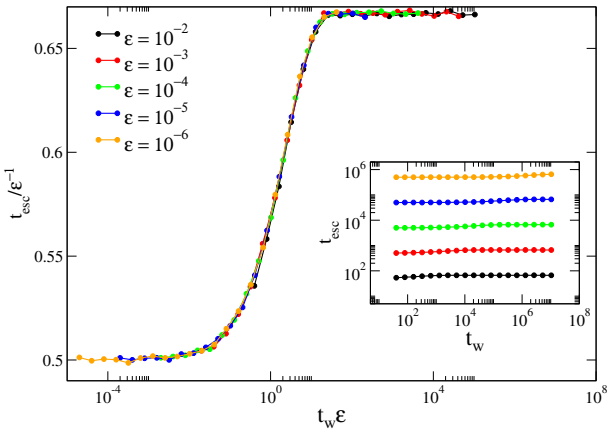

Figure 7. Scaling plot of the average scape time according to Eq. (30) for $\gamma = 2.00$. Inset: raw data. Data corresponds to a network size $N = 10^5$.

indicates that the simple collapse predicted in Eq. (22) cannot be correct, see Fig. 7(inset). We can recover however some form of scaling law for this quantity. Considering a fixed value of ε, the plateau at large t_w is given by the escape time at the stationary state, t^{ss}_{esc}, which is independent of t_w and, from Eq. (7), given by $t^{ss}_{esc} = \int P_\infty(a)/a \; da = \langle a^{-2}\rangle/\langle a^{-1}\rangle \sim \varepsilon^{-1}$, far all γ. On the other hand, for small t_w, t_{esc} is dominated by the deepest traps, and it starts only to increase when the walker has had time to explore a finite fraction of the network, that is, when time is larger than the average trapping time $\langle\tau\rangle$, which, from Eq. (23) is proportional to ε^{-1} for $\gamma > 1$. This reasoning suggest a scaling behavior for the escape time of the form

$$t_{esc}(t_w) = \varepsilon^{-1}\mathcal{G}(t_w\varepsilon). \qquad (30)$$

This scaling form in checked in Fig. 7(main), where we can see that it is quite well satisfied. Incidentally, this scaling form can also be cast in the form valid for $\gamma < 1$, Eq. (22), by simply defining $\mathcal{F}(z) \equiv \mathcal{G}(z)/z$.

6 Conclusions

In this paper we have investigated the temporal relaxation of the simplest dynamical process, namely the random walk, on the class of activity driven temporal networks. We have focused in particular in the case of activated random walks, in which a walker can only leave a node when the latter becomes active. By means of a combination of analytic calculations and numerical experiments, we have shown that, for networks with a power law distribution of activity, the random walk experiences a very slow relaxation towards its steady state. The speed of this relaxation is mainly controlled by the parameter ε, bounding the smallest activity of any node. In the limit of small $\varepsilon \to 0$, the dynamics exhibits aging behavior, characterized additionally by a breaking of time translation symmetry. The aging properties of the random walk are studied by examining different quantities usually applied to characterize aging in glassy systems. Crucially, the aging properties of the random walk depend on the exponent γ in the activity distribution. For $\gamma < 1$, the random walk exhibits a relaxation compatible with "simple" aging, with a unique characteristic time scale given by the average escape time from the least active node, ε^{-1}. In this regime, simple scaling forms for the two-time correlation function and the average escape time can be worked out, starting from a scaling ansatz for the occupation probability $P(a,t_w)$. For $\gamma > 1$, on the other hand, the picture is more complex, with a scaling ruled by several characteristic time scales. This different behavior according to γ can be understood by means of a mapping to Bouchaud's trap model: The case $\gamma > 1$ corresponds in this case to an unphysical representation of the trap model, in which there is a majority of deep traps that induce an extraordinary slow relaxation dynamics.

The results obtained here indicate that, apart form the slowing down already reported in dynamical systems on temporal networks, more complex effects, such as aging, can also be observed. In the present case, in which the temporal network substrate is the activity driven model, aging emerges as the result of the mixing of Poisson activation processes with widely different time scales. A more complex phenomenology is to be expected in real temporal networks with non Poissonian, bursty activation rates.

Acknowledgments

We thank A. Barrat for very helpful comments and discussions. This work has been supported by the CAPES under project No.5511-13-5. RP-S acknowledges financial support from the Spanish MINECO, under projects No. FIS2010-21781-C02-01 and FIS2013-47282-C2-2, and EC FET-Proactive Project MULTIPLEX (Grant No. 317532).

References

1. M.E.J. Newman, *Networks: An introduction* (Oxford University Press, Oxford, 2010)
2. S.N. Dorogovtsev, A.V. Goltsev, J.F.F. Mendes, Rev. Mod. Phys. **80**, 1275 (2008)
3. A. Barrat, M. Barthélemy, A. Vespignani, *Dynamical Processes on Complex Networks* (Cambridge University Press, Cambridge, 2008)
4. R. Cohen, K. Erez, D. ben Avraham, S. Havlin, Phys. Rev. Lett. **85**(21), 4626 (2000)
5. D.S. Callaway, M.E.J. Newman, S.H. Strogatz, D.J. Watts, Phys. Rev. Lett. **85**(25), 5468 (2000)
6. R. Albert, H. Jeong, A. Barabasi, Nature **406**(6794), 378 (2000)
7. R. Pastor-Satorras, C. Castellano, P. Van Mieghem, A. Vespignani (2014), `e-print arXiv:1408.2701`
8. P. Holme, J. Saramäki, Physics Reports **519**, 97 (2012)
9. M. Jackson, *Social and Economic Networks* (Princeton University Press, Princeton, 2010)
10. J.G. Oliveira, A.L. Barabasi, Nature **437**(7063), 1251 (2005)
11. J.P. Onnela, J. Saramäki, J. Hyvönen, G. Szabó, D. Lazer, K. Kaski, J. Kertész, A.L. Barabási, Proceedings of the National Academy of Sciences **104**(18), 7332 (2007)
12. C. Cattuto, W. Van den Broeck, A. Barrat, V. Colizza, J.F. Pinton, A. Vespignani, PLoS ONE **5**, e11596 (2010)
13. A. Vazquez, B. Rácz, A. Lukács, A.L. Barabási, Phys. Rev. Lett. **98**, 158702 (2007)
14. H.H. Jo, J.I. Perotti, K. Kaski, J. Kertész, Phys. Rev. X **4**, 011041 (2014)
15. M. Kivela, R. Kumar Pan, K. Kaski, J. Kertesz, J. Saramaki, M. Karsai, J. Stat. Mech. p. P03005 (2012)
16. J. Stehle, N. Voirin, A. Barrat, C. Cattuto, V. Colizza, L. Isella, C. Regis, J.F. Pinton, N. Khanafer, W. Van den Broeck et al., BMC Medicine **9**(87) (2011)
17. N. Fujiwara, J. Kurths, A. Díaz-Guilera, Physical Review E **83**(2), 025101 (2011)
18. G.H. Weiss, *Aspects and Applications of the Random Walk* (North-Holland Publishing Co., Amsterdam, 1994)
19. M. Starnini, A. Baronchelli, A. Barrat, R. Pastor-Satorras, Phys. Rev. E **85**, 056115 (2012)
20. N. Perra, A. Baronchelli, D. Mocanu, B. Gonçalves, R. Pastor-Satorras, A. Vespignani, Physical Review Letters **109**(23), 238701 (2012)
21. B. Ribeiro, N. Perra, A. Baronchelli, Scientific Reports **3**, 3006 (2013), ISSN 2045-2322
22. T. Hoffmann, M.A. Porter, R. Lambiotte, Physical Review E **86**(4), 046102 (2012)
23. N. Perra, B. Gonçalves, R. Pastor-Satorras, A. Vespignani, Scientific Reports **2**, srep00469 (2012)
24. M. Henkel, M. Pleimling, *Non-equilibrium phase transition: Ageing and Dynamical Scaling far from Equilibrium* (Springer Verlag, Netherlands, 2010)
25. J. P. Bouchaud, J. Phys. I France **2**(9), 1705 (1992)
26. C. Monthus, J.P. Bouchaud, Journal of Physics A: Mathematical and General **29**(14), 3847 (1996)
27. M. Starnini, R. Pastor-Satorras, Physical Review E **87**(6), 062807 (2013)
28. M.E.J. Newman, Proc. Natl. Acad. Sci. USA **98**, 404 (2001)
29. M.E.J. Newman, Physical Review E **64** (2001)
30. A. Baronchelli, A. Barrat, R. Pastor-Satorras, Phys. Rev. E **80**(2), 020102 (2009)
31. P. Moretti, A. Baronchelli, A. Barrat, R. Pastor-Satorras, Journal of Statistical Mechanics: Theory and Experiment **2011**, P03032 (2011)
32. M. Abramowitz, I.A. Stegun, *Handbook of mathematical functions.* (Dover, New York, 1972)